Inhibition of Lipolysis by Palmitate, H_2O_2 and the Sulfonylurea Drug, Glimepiride, in Rat Adipocytes Depends on cAMP Degradation by Lipid Droplets

Günter Müller,* Susanne Wied, Sabine Over, and Wendelin Frick

Sanofi-Aventis Pharma, Therapeutic Department Metabolism, 65926 Frankfurt am Main, Germany

Received July 18, 2007; Revised Manuscript Received October 5, 2007

ABSTRACT: The release of fatty acids and glycerol from lipid droplets (LD) of mammalian adipose cells is tightly regulated by a number of counterregulatory signals and negative feedback mechanisms. In humans unrestrained lipolysis contributes to the pathogenesis of obesity and type II diabetes. In order to identify novel targets for the pharmacological interference with lipolysis, the molecular mechanisms of four antilipolytic agents were compared in isolated rat adipocytes. Incubation of the adipocytes with insulin, palmitate, glucose oxidase (for the generation of H_2O_2) and the antidiabetic sulfonylurea drug, glimepiride, reduced adenylyl cyclase-dependent, but not dibutyryl-cAMP-induced lipolysis as well as the translocation of hormone-sensitive lipase and the LD-associated protein, perilipin-A, to and from LD, respectively. The antilipolytic activity of palmitate, H_2O_2 and glimepiride rather than that of insulin was dependent on rolipram-sensitive but cilostamide-insensitive phosphodiesterase (PDE) but was not associated with detectable downregulation of total cytosolic cAMP and insulin signaling *via* phosphatidylinositol-3 kinase and protein kinase B. LD from adipocytes treated with palmitate, H_2O_2 and glimepiride were capable of converting cAMP to adenosine *in vitro*, which was hardly observed with those from basal cells. Conversion of cAMP to adenosine was blocked by rolipram and the 5′-nucleotidase inhibitor, AMPCP. Immunoblotting analysis revealed a limited salt-sensitive association with LD of some of the PDE isoforms currently known to be expressed in rat adipocytes. In contrast, the cAMP-to-adenosine converting activity was stripped off the LD by bacterial phosphatidylinositol-specific phospholipase C. These findings emphasize the importance of the compartmentalization of cAMP signaling for the regulation of lipolysis in adipocytes, in general, and of the involvement of LD-associated proteins for cAMP degradation, in particular.

The major physiological role of white adipose tissue fat stores is to supply lipid energy when it is needed by other tissues. This is achieved by a highly regulated catabolic pathway, lipolysis, whereby the TAG stored in the adipocyte LD[1] is hydrolyzed into FA and glycerol which are subsequently released into the plasma. Excessive lipolysis contributes to high circulating levels of FA and the development of dyslipidemia resulting in lipotoxicity and insulin resistance of peripheral tissues as observed in the metabolic syndrome and in type II diabetes (*1*). Pharmacological targeting of lipolysis can be envisaged at distinct levels of the lipolytic cascade (*2*). Drugs acting at the receptor level, such as nicotinic acid, and direct inhibitors of lipases have been tested as putative insulin-sensitizing or blood glucose-lowering agents. However, so far none of them proved to be efficious due to a variety of reasons (e.g., receptor desensitization, inadequate plasma FA lowering). Therefore, elucidation of mechanisms for receptor-independent regulation of lipolysis may lead to novel targets for diabetes therapy.

A number of receptor-independent antilipolytic stimuli have been described during the past decades, among them H_2O_2 (*3*, *4*), free FA (*5*) and the antidiabetic sulfonylurea drug, glimepiride (*6*−*8*). However, the molecular mechanisms underlying the observed lipolysis inhibition in isolated and cultured rodent and human adipocytes remained elusive so far. It is generally assumed that the majority of antilipolytic stimuli act *via* lowering of cytosolic cAMP during either inhibition of plasma membrane adenylate cyclase (e.g., nicotinic acid) or stimulation of microsomal PDEs (e.g., insulin) (*9*). In lipolytically induced adipocytes cAMP levels in the cytosol become elevated leading to activation of PKA. Upon phosphorylation by PKA, HSL is translocated from the cytosol to the surface of LD (*10*), whereas simultaneously perilipin, associated with the LD surface, is modified for more efficient docking of HSL (*11*). These processes which rapidly initiate TAG cleavage by HSL are reversed upon degradation of cAMP by activated PDEs.

The activation of PDEs *via* receptor-mediated pathways, such as insulin signaling, is rather complex. Upon activation of the IR and the resulting tyrosine phosphorylation of intracellular substrate proteins, such as IRS-1, the lipid kinase activity of the PI3′K is activated. The phosphatidylinositol-3-phosphate formed at the plasma membrane interacts with and thereby activates PKB, which then phosphorylates and stimulates PDE3B (*12*−*16*). The central role of PDE3B for

* To whom correspondence should be addressed: Sanofi-Aventis Pharma Germany GmbH, TD Metabolism, Industrial Park Höchst, Bldg. H821, 65926 Frankfurt am Main, Germany; phone, +4969-305-4271; fax, +4969-305-81901; e-mail, Guenter.Mueller@sanofi-aventis.com.

[1] Abbreviations: ADA, adenosine deaminase; (c)AMP, (cyclic) adenosine monophosphate; D/TAG, di/triacylglycerol; DIGs, detergent insoluble glycolipid-enriched microdomains; FA, fatty acids; GO, glucose oxidase; HSL, hormone-sensitive lipase; IBMX, isobutylmethylxanthine; IR, insulin receptor; LD, lipid droplets; MAPK(K), mitogen-activated protein kinase (kinase); 5′-Nuc, 5′-nucleotidase; PDE, phosphodiesterase; PI3′K, phosphatidylinositol-3 kinase; PKA/B, protein kinase A/B; SDS−PAGE, sodium dodecylsulfate polyacrylamide gel electrophoresis.

10.1021/bi701413t CCC: $40.75
Published on Web 01/11/2008

insulin inhibition of lipolysis is exemplified by the excessive and sustained lipolysis in adipocytes from PDE3B knockout mice (*17*) or rats treated with a PDE3B-specific inhibitor (*16*) and in 3T3-L1 adipocytes with downregulated PDE3B expression upon long-term treatment with tumor necrosis factor-α (*18*). The antilipolytic activities of H_2O_2, FA and glimepiride may also involve stimulation of PDE3B relying in part on components of the insulin signaling cascade. This assumption was based on the known direct inhibition of protein tyrosine phosphatase 1B, the major IR dephosphorylating and inactivating enzyme by H_2O_2 (*19*) and the known stimulation of IRS-1 phosphorylation and activation by the nonreceptor tyrosine kinase, $pp59^{Lyn}$, in response to glimepiride (*7*, *8*). Both mechanisms would finally result in upregulation of PDE3B along the insulin signaling cascade and are compatible with the well-documented broad insulin-mimetic activity of both H_2O_2 (*20*) and glimepiride (*7*, *8*). Since FA have been reported to cause the production of H_2O_2 (*3*−*5*) driven by mitochondrial β-oxidation in various cell types, the activation of PDE3B may also underly the antilipolytic activity of FA. In addition, impaired cAMP production from glycolytic ATP, the amount of which may be lowered due to the fostered β-oxidation, has been proposed as PDE3B-independent antilipolytic mechanism of FA (*21*, *22*). However, the series of events leading to lipolysis inhibition by FA, H_2O_2 and glimepiride in adipocytes remained to be unraveled on an experimental basis.

The diversity of effects mediated by cAMP is generally thought to rely on both the dynamic regulation (synthesis and degradation) and localized action of this highly diffusible messenger. Compartmentalization of cAMP synthesis and degradation to discrete cellular regions is thought to arise from the localization of G protein-coupled receptors with adenylate cyclases and PDEs, respectively. With regard to the spatiotemporal control of PDEs, it has recently been found in T-cells that local increases in PDE4 activity in plasma membrane areas upon T-cell receptor and CD28 engagement can play a key role in tuning intracellular activation-induced gradients of cAMP (*23*). The mechanisms by which PDE4 are recruited to plasma membrane areas upon T-cell activation remain to be elucidated, but protein−protein interactions involving the scaffolding protein, β-arrestin, seem to play a critical role in the transient and local accumulations of cAMP at plasma membrane areas (*24*−*26*).

Despite growing evidence for the importance of compartmentalization of cAMP degradation by PDEs, experimental support is lacking so far for their role in the regulation of lipolysis in adipocytes. Here we present evidence that downregulation of lipolysis by three structurally completely different agents, H_2O_2, palmitate and glimepiride, depends on the local increase in cAMP-degrading activities (including PDE) at LD which involves lipid−lipid rather than protein−protein interactions. This antilipolytic mechanism, which apparently leads to localized rather than total decreases in cytosolic cAMP, is clearly different from that engaged by insulin and emphasizes the critical role of dynamic and regulated compartimentalization of cAMP degradation for signaling *via* cAMP, in general, and inhibition of lipolysis, in particular.

MATERIALS AND METHODS

Materials. Human recombinant insulin, glimepiride (trade name Amaryl), glibenclamide, tolbutamide, glimepiride M1 and the (G)PI-PLC inhibitor GPI-2350 were made available by the biotechnological production and medicinal chemistry synthesis departments of Sanofi-Aventis Pharma (Frankfurt; Germany). Wortmannin, BATC (β-amidotaurocholate), Sp-8-bromo-adenosine 3′,5′-cyclic monophosphorothioate (Sp-8-Br-cAMPS), OPC3911, cilostamide, dipyridamole, rolipram, vinpocetine and zaprinast were delivered by Calbiochem (Darmstadt, Germany). PKB inhibitor 124005 was bought from EMD Biosciences (San Diego, CA). Protein A-Sepharose were provided by Pharmacia/LKB (Freiburg, Germany). 5′-Nuc (*Crotalus atrox*), adenosine 5′-[α,β-methylene]diphosphate (AMPCP), forskolin (*Coleus forskohlii*), IBMX, PD98059 and N^6,2′-O-dibutyryladenosine 3′5′-cyclic monophosphate (dibutyryl-cAMP) were from Sigma/Aldrich (Deisenhofen, Germany). GO, ADA and premixed protease (complete EASYpack) and phosphatase (PhosSTOP) inhibitor cocktails (1 tablet each for 10 mL) were purchased from Roche Molecular Biochemicals (Mannheim, Germany). Collagenase (Worthington, CLS, type I, 250 units/mg) was delivered by Biochrom. HNMPA-$(AM)_3$ (hydroxy-2-naphthalenylmethyl-phosphonic acid−tris acetoxymethylester) was provided by Biomol (Hamburg, Germany). Lipids were purchased from Avanti Polar Lipids. Precast gels were from Novex (San Diego, CA). Polyvinylidene difluoride membranes (Immobilon-P) were obtained from Millipore (Eschborn, Germany). Rats were provided by Charles-River Laboratories and handled in agreement with the German Animal Protection Law. All other materials were obtained as described previously (*27*−*29*).

Preparation and Incubation of Rat Adipocytes. Adipocytes isolated by collagenase digestion from epididymal fat pads of male Sprague Dawley rats (140−160 g, fed ad libitum) according to published procedures (*30*) were suspended in 0.5 mL or 25 mL (for preparative purposes) of KRH (140 mM NaCl, 4.7 mM KCl, 2.5 mM $CaCl_2$, 1.2 mM $MgSO_4$, 1.2 mM KH_2PO_4, 20 mM Hepes/KOH, pH 7.4, containing 2% (w/v) BSA, 100 μg/mL gentamycin, 1 mM sodium pyruvate and 5.5 mM D-glucose) at 5×10^5 cells/mL in a shaking water bath (100 cycles/min, 37 °C) under constant bubbling with 5% CO_2/95% O_2 for the incubation with insulin, palmitate, GO and glimepiride prior to the stimulation of lipolysis by isoproterenol, ADA, forskolin or dibutyryl-cAMP as indicated. The preparation of stock solutions of insulin, palmitate and glimepiride coupled to BSA has been outlined previously (*34*). Recombinant GO in 10 mM phosphate buffer (pH 7.4) at 10 U/mL was diluted in KRH immediately before use. Stock solution of inhibitors were made in DMSO at 10 mM. The final DMSO concentration was kept constant at 0.5% at any inhibitor concentration. Incubation of the adipocytes in primary culture at 5.5 mM glucose was performed as described previously (*31*).

Determination of H_2O_2. Levels of H_2O_2 were determined with 150-μL aliquots of the adipocyte suspensions. Medium was separated from the cells by centrifugation through 300-μL cushions of dinonylphthalate and assayed for H_2O_2 by the chromogenic method of Ngo and Lenhoff (*32*). Cell breakage and the release of H_2O_2-degrading enzymes were monitored by determining lactate dehydrogenase release and

by following the disappearance of exogenously added H_2O_2 (80 μM), respectively. Alternatively, H_2O_2 generation was detected by reduction of NBT which leads to a relatively stable product detectable at 560 nm for at least 120 min following initiation. The assay was performed by incubating (2 h, 37 °C) 250-μL aliquots of the adipocyte suspensions with 0.2% NBT and 5.5 mM glucose in the absence or presence of GO under 5% CO_2/95% O_2. After centrifugation of the incubation mixtures (500*g*, 2 min, 15 °C), the infranatants were removed from the floating adipocytes by suction and 100-μL portions were supplemented with formazan dissolved in 100 μL of 50% acetic acid. Absorbance was determined at 560 nm in a microtiter plate reader (Spectromax Plus, Molecular Devices, USA).

Preparation of LD, Microsomes and Cytosol. LD were prepared according to published procedures (*33*, *34*) with the following modifications: After the incubation, adipocytes in 25 mL of incubation mixture were washed two times with KRH by flotation (200*g*, 1 min, 15 °C) and removal of the infranatant by suction and then homogenized in 4 mL of buffer L (25 mM Tris/HCl, pH 7.4, 250 mM sucrose, 5 mM NaF, 10 mM $NaPP_i$, 1 mM Na_3VO_4, 1 mM EDTA, 5 μg/mL pepstatin, 20 μg/mL leupeptin, 1 mM benzamidine, 0.5 mM PMSF) supplemented with complete protease and phosphatase inhibitor cocktail tablets (Roche) at 15 °C. The homogenate was centrifuged (500*g*, 5 min, 15 °C). For the preparation of LD, 1-mL portions of the supernatant were combined with 1.5 mL of 65% sucrose (w/v) each and poured into 5-mL centrifuge tubes. 1.5 mL of 10% sucrose (w/v) was then layered on top of the sucrose cushion. The tube was filled to capacity with buffer L lacking sucrose. The gradients were centrifuged (172000*g*, 1 h, 15 °C) and then allowed to coast to rest. The floating fraction of LD was visualized as the upper white layer of the gradient, isolated by suction with a syringe (0.5−0.8 mL) and washed two times with 4 mL of buffer L each. LD were reisolated from incubation mixtures by 10-fold dilution with buffer L, subsequent centrifugation (12000g, 2 min, 15 °C) and final removal of the upper lipid layer by suction. For incubation, LD were suspended in 5 volumes of buffer L (50−100 μL) under sonication in bath ultrasonifier (5 × 30-s periods with 30-s intervals, 15 °C, maximum power) and then treated as indicated. Subsequently, LD were reisolated by sucrose gradient centrifugation (see above) and suspended in the desired volume. For preparation of cytosol and microsomes, the infranatant of the gradient centrifugation was diluted with three volumes of buffer L and then recentrifuged (100000*g*, 1 h, 4 °C). The supernatant was used as cytosol, the pellet (= microsomes) was washed once with buffer L and then suspended in buffer L at 2−4 mg of protein/mL.

The identity and purity of the LD was studied as described previously (*34*). Briefly, when the top fraction of the sucrose gradient, which yielded a layer of white matter, was stained with Oil red O, a dye specific for neutral lipids, a number of red-colored spheres were observed under a microscope. Thin layer chromatography of the lipids extracted from the gradient fractions revealed almost quantitative recovery of TAG, cholesteryl ester, cholesterol and phospholipids in the top fraction. In agreement with previous findings (*35*, *36*), LD from control adipocytes contained high contents of cholesteryl esters, TAG and an unknown neutral lipid species that migrated between TAG and cholesteryl esters as well as small amounts of DAG, cholesterol and total phospholipids (data not shown). Judging from the protein profile (Coomassie blue), the top fraction contained a very small amount of protein, only. When larger amounts of the top fraction were loaded, about 20 proteins were detected with five being abundant. This protein composition was clearly distinct from that of total cell lysate (data not shown). Lactate dehydrogenase activity, calnexin, integrin and golgin, markers for the cytosol, endoplasmic reticulum, plasma membrane and Golgi apparatus, respectively, were hardly or not detected in the top fraction. Thus, it is unlikely that the lipids and proteins in the top fraction were contaminants from the denser cytosolic or membrane fractions.

Protein Extraction from LD. For denaturating conditions, the washed LD were suspended in 4-fold Laemmli sample buffer containing 20% SDS (typically 50 μL per 10 μL of LD) by incubation (10 min, 65 °C). After centrifugation (10000*g*, 5 min, 25 °C), the infranatant was withdrawn by suction and proteins were precipitated under denaturing conditions. For native conditions, the washed LD were suspended in buffer lacking sucrose and containing 1 M NaCl, 0.2% TX-100, 1.5% BATC and 60 mM octylglucoside, then treated in a bath sonicator (5 × 30-s periods with 30-s intervals, 15 °C, maximum power) and incubated (15 min, 37 °C). After centrifugation (10000*g*, 5 min), the infranatant proteins were precipitated under native conditions.

Protein Precipitation. For native conditions, protein samples were supplemented with BSA (final concentration 0.1 mg/mL) and then PEG6000 (25% in Mops/KOH, pH 7.4, 0.5 mM DTT, 0.5 mM $MgCl_2$, final concentration 12%). After incubation (1 h, on ice) and centrifugation (12000*g*, 10 min, 4 °C), precipitated proteins were washed with 0.5% PEG6000 and then dissolved in 20 mM Tris/HCl (pH 7.4), 1 mM EDTA, 0.5 mM DTT, 20 mM octylglucoside, 0.1% BATC and protease and phosphatase inhibitors at 0.1−1 mg protein/mL. For denaturing conditions, proteins samples were incubated (1 h, on ice) with 5% trichloro-acetic acid and centrifuged (12000*g*,10 min, 4 °C). Precipitated proteins were washed with cold acetone, dried and then solubilized in 2-fold Laemmli sample buffer (2−4 mg/mL).

Extraction and Determination of LD Lipids. For determination of total lipid mass, lipids were extracted from LD into methanol by a modification of the Bligh and Dyer method (*37*) in which methanol was replaced with 2-propanol. Monophasic extracts were partitioned into two phases, and the organic layer was washed three times with 1 M KCl (*38*). Total lipid mass was estimated gravimetrically after removing solvent under a gentle stream of N_2 gas. For TLC analysis, lipids were extracted from LD using methanol/acetone (1/1, by vol.). The solvent was removed by N_2 gas, and the lipids were dissolved in methanol and spotted onto TLC plates (silica gel 60) developed first with chloroform/methanol/acetic acid (98/2/1, by volume) and then with hexane/diethyl ether/acetic acid (80/20/1, by volume). The plates were soaked in 8% phosphoric acid containing 3% cupric acetate. Lipid classes were visualized by heating at 130 °C. For quantitative evaluation, the plates were scanned and the densities of the lipid spots were measured with standard imaging software. Standard curves were created using various amounts of standard triolein, cholesteryl oleate, cholesterol, dioleoyl glycerol and phosphatidylcholine spotted and developed under the same conditions on the same plates.

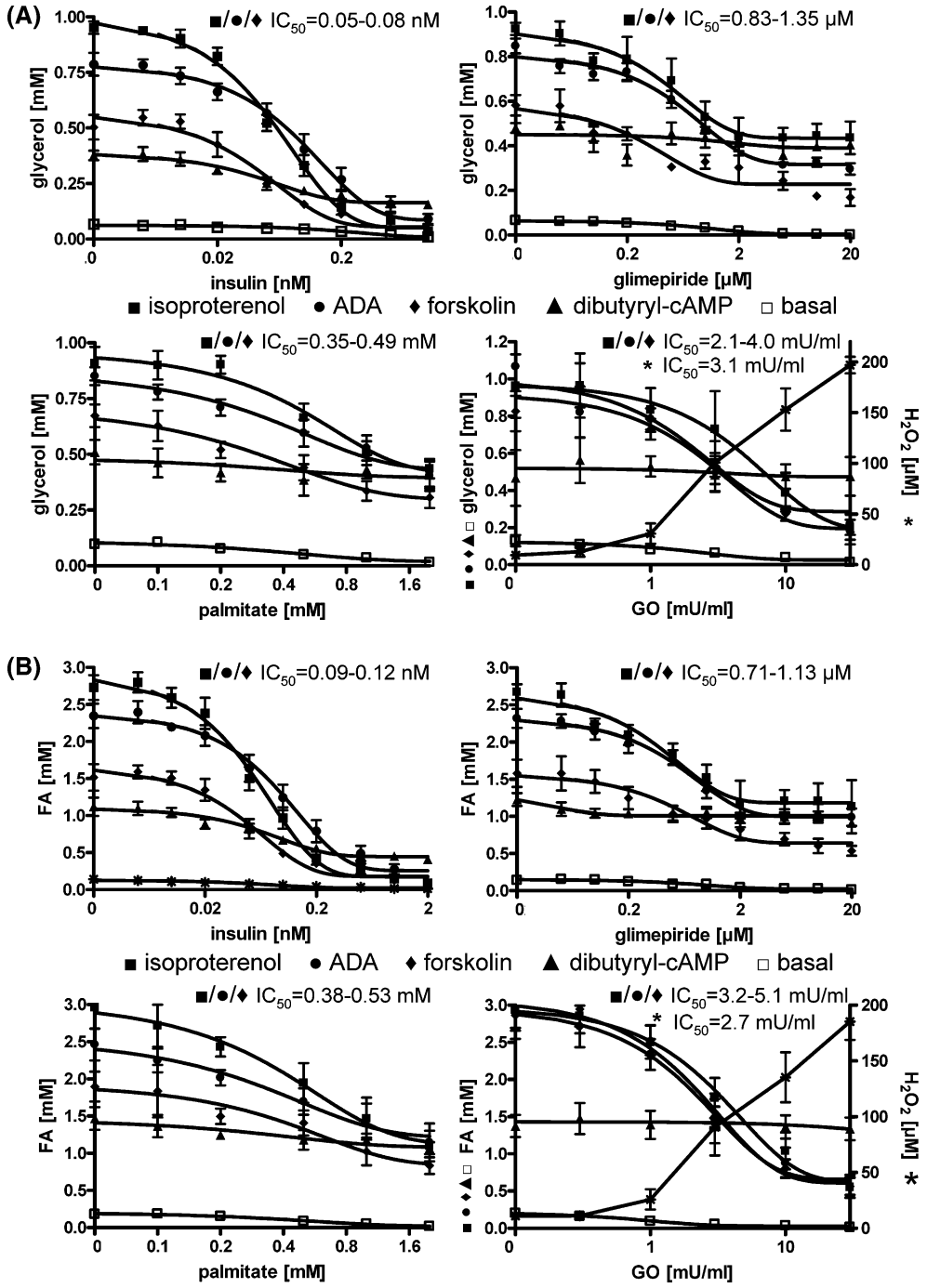

FIGURE 1: Effect of insulin, glimepiride, palmitate and GO on the isoproterenol-, forskolin-, dibutyryl-cAMP- and ADA-stimulated release of glycerol and FA. Isolated rat adipocytes were incubated (37 °C) in the absence or presence of increasing concentrations of insulin (5 min), glimepiride (60 min), palmitate (120 min) and GO (20 min) prior to the addition of isoproterenol (final concentration 1 μM), ADA (1 U/mL), dibutyryl-cAMP (1 mM), forskolin (25 μM) or buffer alone (basal) as indicated. After further incubation (2 h), the medium was separated from the adipocytes and analyzed for glycerol (panel A) and FA (panel B) released as well as for H_2O_2 generated by GO action using the chromogenic (panel A) or NBT (panel B) method as described in Materials and Methods. (Means ± SD, $n = 4$ adipocyte preparations with incubations in triplicate each; significant differences ($p < 0.05$) for isoproterenol-, ADA- and forskolin-induced lipolysis with insulin ≥ 0.02 nM, glimepiride ≥ 0.5 μM, palmitate ≥ 0.5 mM and GO ≥ 2 mU/mL as well as for dibutyryl-cAMP-induced lipolysis with insulin ≥ 0.1 nM compared to the absence of the agents.)

SDS−PAGE and Immunoblotting. SDS−PAGE and immunoblotting using chemiluminescent detection were performed as outlined previously (*28*, *29*) with the following primary antibodies: Anti-HSL (1:100) raised in rabbits against a synthetic peptide, GPRLELRPRPQQAPRS, corresponding to rat HSL amino acids 326−341 and delivered by Biotrend (Cologne, Germany); anti-perilipin-A (1:1000) raised in guinea pigs against a synthetic peptide corresponding to the N-terminal region of human perilipin-A (GP29); anti-ADRP (monoclonal, 1:250) and anti-TIP47 (monoclonal, 1:400) delivered by Progen Biotechnik (Heidelberg, Germany); anti-caveolin-1 (1:2000) and anti-vimentin (1:750) raised in rabbits and delivered by BD Transduction Laboratories (San Jose, USA); anti-PDE isoforms (monoclonal, 1:200) delivered by Scottish Biomedicals (Glasgow, U.K.). Chemiluminescent detection (ECL, Amersham-Buchler) and

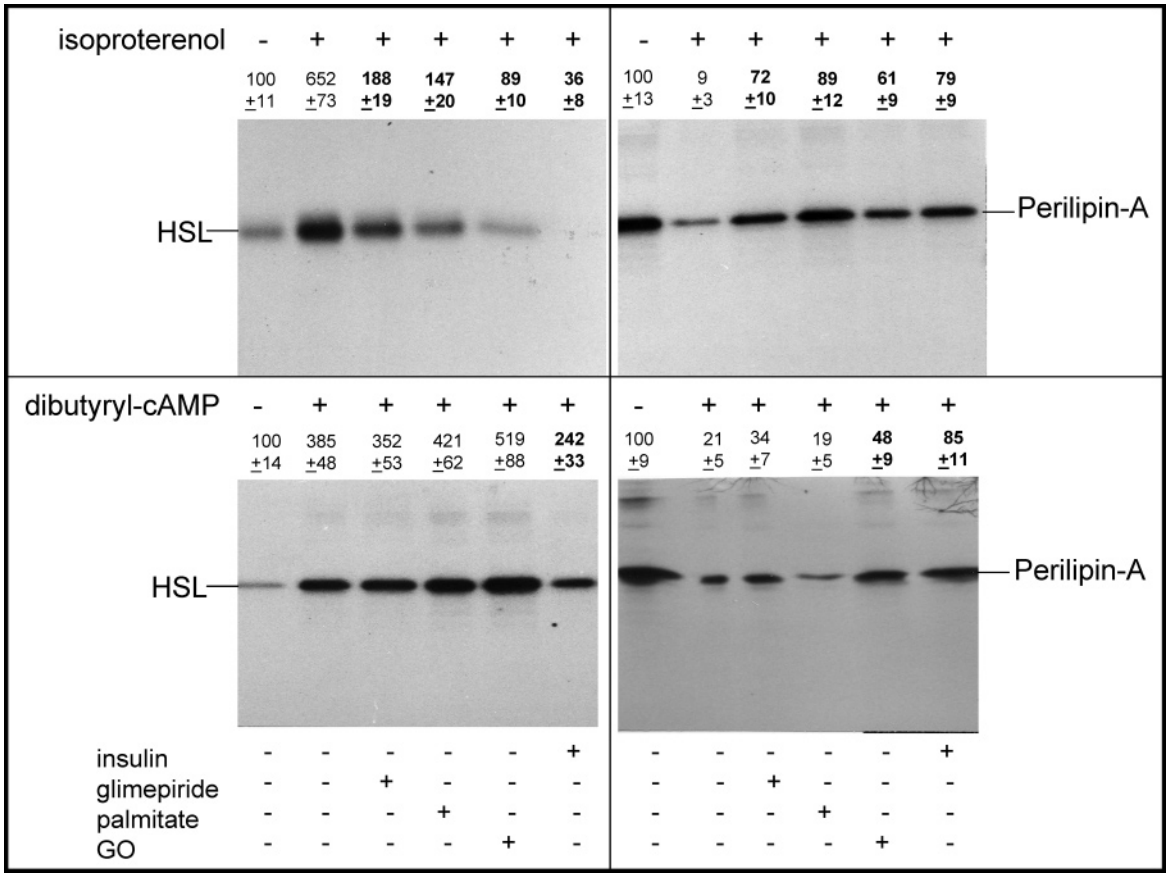

FIGURE 2: Effect of insulin, glimepiride, palmitate and GO on the isoproterenol- and dibutyryl-cAMP-stimulated association of HSL and perilipin with LD. Isolated rat adipocytes were incubated (37 °C) in the absence or presence of insulin (0.5 nM, 5 min), glimepiride (10 μM, 60 min), palmitate (1 mM, 120 min) and GO (10 mU/mL, 20 min) prior to the addition of isoproterenol (final concentration 1 μM) or dibutyryl-cAMP (1 mM) or buffer alone. After further incubation (20 min), the adipocytes were separated from the medium and used for the preparation of LD. Proteins were extracted and precipitated under denaturing conditions and finally immunoblotted for HSL and perilipin-A as described in Materials and Methods. The specificity of the HSL antibodies was tested with recombinant human HSL which resulted in labeling of a single 82-kDa crossreactive polypeptide. Lumiimages of a typical SDS−PAGE are shown. Quantitative evaluation by lumiimaging is given with the amount of HSL and perilipin-A recovered with LD from basal untreated adipocytes set at 100. (Means ± SD, $n = 3$ adipocyte preparations with immunoblotting in duplicate; bold numbers indicate significant differences compared to the isoproterenol- or dibutyryl-cAMP-induced HSL or perilipin-A translocation in the absence of agent at $p < 0.01$.)

quantitative evaluation of the lumiimages was performed using the Roche Lumiimager system and software (Roche, Mannheim, Germany) as described earlier (*39*).

Determination of Cytosolic cAMP Levels. cAMP levels were determined from 50-μL portions of cytosol using a commercially available competitive ELISA kit with a cAMP-alkaline phosphatase tracer according to the instructions of the manufacturer Biotrend (Cologne, Germany) in the wells of a 96-well plate precoated with mouse anti-rabbit IgG. After addition of cAMP antiserum and equilibration, the plate was washed. Thereafter, the alkaline phosphatase substrate, *p*-nitrophenyl phosphate, was added. Product formation of this enzymic reaction was monitored at 412 nm. The assay permits cAMP measurements within the range of 3−3000 pmol/mL, typically with a detection limit of 10 nM, intra-assay and inter-assay precisions of 5−20%, and cross-reactivities with AMP and adenosine of less than 0.05%.

Conversion of cAMP to Adenosine. Reactions were started by the addition of [^{14}C]cAMP (final concentration 20 μM, 3 $\times$ 10^5 cpm/well) to 25 μL of LD or the corresponding amount of extracted protein or microsomes in buffer L in a total volume of 100 μL in the wells of 96-well microtiter plates. Samples (10 μL each) were withdrawn at 0, 30, and 60 min and then analyzed for radiolabeled adenosine by TLC on Kodachrome microcrystalline cellulose plates and subsequent phosphorimaging. Rates of adenosine generation were linear within this time period, and the maximal amount of degraded cAMP never exceeded 10%. For the analysis of microsomes, purified 5′-Nuc (0.05 unit, *Crotalus atrox*) was included into the reaction mixture.

Miscellaneous. Published procedures were used for the determination of glycerol and FA release from adipocytes (*40*, *41*) and the preparation of DIGs (*29*). Protein concentration was determined by using the BCA method (Pierce) with BSA as calibration standard. Concentration−response curves were fitted by using the GraphPad Prism 4.03 software. Figures of lumiimages were constructed using the Adobe Photoshop software (Adobe Systems, Mountain View, CA).

RESULTS

Inhibition of Lipolysis by Insulin, H_2O_2, Palmitate and Glimepiride in Rat Adipocytes Depends on Different Molecular Mechanisms. As a first step in differentiating the antilipolytic activities of H_2O_2, palmitate, glimepiride and insulin, their effects on lipolysis induced by either receptor/adenylyl cyclase-dependent or independent upregulation of the cAMP signaling cascade was investigated. For this,

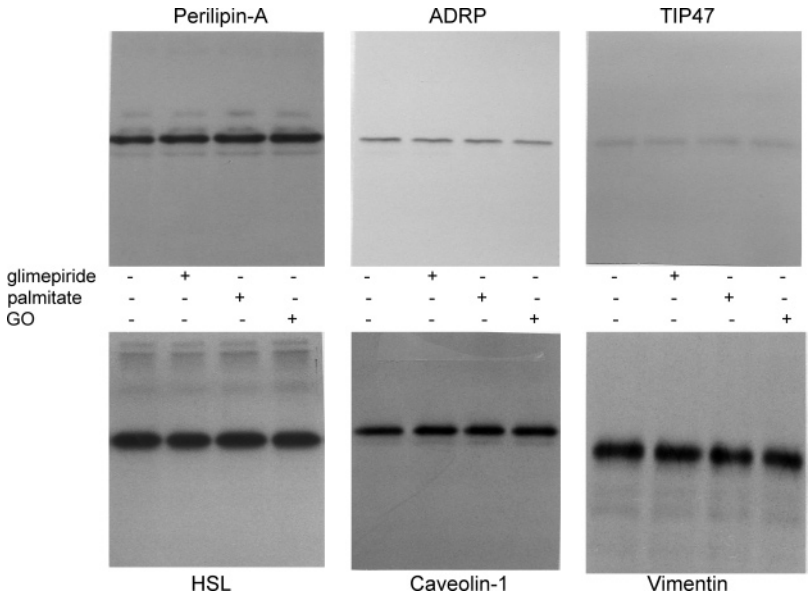

FIGURE 3: Effect of glimepiride, palmitate and GO on the protein composition of LD. Isolated rat adipocytes were incubated (37 °C) in the absence or presence of glimepiride (10 μM, 60 min), palmitate (1 mM, 120 min) or GO (10 mU/mL, 20 min) and then separated from the medium for the preparation of LD. Proteins were extracted from the LD, precipitated under denaturing conditions and immunoblotted for perilipin-A, ADRP, TIP47, HSL, caveolin-1 and vimentin. Lumiimages from a experiment are shown repeated once with similar results.

Table 1: Effect of Insulin, Glimepiride, Palmitate and GO on the Lipid Composition of LD[a]

lipolysis stimulator	lipolysis inhibitor	CholE	LX	TAG	DAG/Chol	PL
basal		28 ± 3	18 ± 5	49 ± 10	0.8 ± 0.3	1.9 ± 0.6
isoproterenol		22 ± 4	13 ± 2	44 ± 5	1.4 ± 0.2	2.0 ± 0.4
	insulin	29 ± 5	20 ± 3	47 ± 8	0.7 ± 0.3	1.6 ± 0.8
	glimepiride	30 ± 7	22 ± 5	51 ± 11	0.8 ± 0.4	2.2 ± 0.8
	palmitate	32 ± 7	19 ± 6	53 ± 10	0.9 ± 0.4	1.8 ± 0.6
	GO	33 ± 8	17 ± 5	52 ± 12	1.1 ± 0.5	2.4 ± 1.4
dibutyryl-cAMP		20 ± 3	14 ± 4	40 ± 6	1.3 ± 0.4	2.2 ± 0.7
	insulin	30 ± 4	19 ± 3	51 ± 7	0.7 ± 0.3	2.7 ± 0.9
	glimepiride	22 ± 4	11 ± 3	39 ± 6	0.6 ± 0.2	2.1 ± 0.7
	palmitate	19 ± 5	12 ± 4	38 ± 9	1.0 ± 0.4	1.8 ± 0.5
	GO	23 ± 4	15 ± 3	42 ± 7	0.9 ± 0.3	1.8 ± 0.6

[a] Isolated rat adipocytes were incubated (37 °C) in the absence or presence of insulin (0.5 nM, 5 min), glimepiride (10 μM, 60 min), palmitate (1 mM, 120 min) and GO (10 mU/mL, 20 min) prior to the addition of isoproterenol (final concentration 1 μM) or dibutyryl-cAMP (1 mM) or buffer alone (basal). After further incubation (2 h), the adipocytes were separated from the medium for the preparation of LD. Lipids were extracted from the LD, then separated by TLC and finally visualized with iodine vapor. The solvent system resolved cholesteryl ester (CholE), the unknown lipid species (LX), TAG and diacylglycerol (DAG)/cholesterol (Chol) but left phospholipids (PL) as revealed by comparison with lipid standards run in parallel on the same plate. The relative amounts (%) of the major lipid classes were quantitatively evaluated by densitometric scanning of the plates using ImageQuant software and comparison with TLC standards. LX was quantified against a TAG standard curve. (Means ± SD, n = 3 adipocyte preparations with determinations in duplicate.)

lipolysis was induced in isolated rat adipocytes by maximally effective concentrations of isoproterenol (by 14-fold above basal) for stimulation of the G_s-protein-coupled β-adrenoceptors, ADA (by 12-fold above basal) for deactivation of the G_i-protein-coupled A1-adenosine receptor in the course of adenosine removal, forskolin (by 8-fold above basal) for direct receptor-independent stimulation of adenylyl cyclase or dibutyryl-cAMP (by 5-fold above basal) for direct activation of PKA. Treatment of adipocytes with insulin, palmitate, glimepiride or GO (for the generation of H_2O_2) diminished the isoproterenol-, ADA- and forskolin-induced release of glycerol (Figure 1A) and FA (Figure 1B) into the incubation medium in concentration-dependent and significant fashion by up to 80−90%, 45−55%, 55−65% and 70−80%, respectively. For each antilipolytic agent, the IC_{50}-values for inhibition of glycerol and FA release were similar and did not differ significantly between isoproterenol, forskolin and ADA stimulation. In contrast, the glycerol and FA release triggered by nonhydrolyzable dibutyryl-cAMP was not affected significantly by glimepiride, palmitate and GO, and moderately but significantly reduced in response to insulin (IC_{50} = 0.1 nM). Basal lipolysis (absence of lipolytic stimulus) was low with the incubation conditions employed and reduced further and nonsignificantly to up to the detection limit of glycerol and FA in response to all four agents (Figure 1).

The concentrations of H_2O_2 generated by GO action (1−100 mU/mL) in the incubation medium of the rat adipocytes and determined by two different methods were 30−200 μM (Figure 1) and thus within the range previously reported to be generated in the medium of 3T3-L1 adipocytes (*42*) and to exert potent insulin-mimetic activity *in vitro* (*19*). GO-induced elevation in H_2O_2 and inhibition of lipolysis was not observed during the concomitant presence of catalase

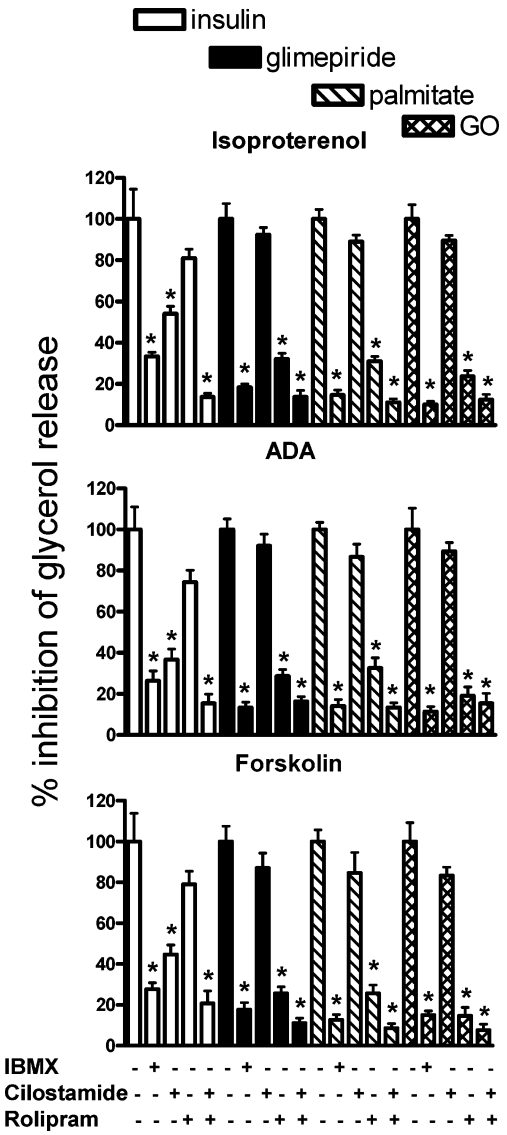

FIGURE 4: Effect of PDE inhibition on blockade of the isoproterenol-, ADA-, and forskolin-stimulated lipolysis by insulin, glimepiride, palmitate and GO. Isolated rat adipocytes were incubated (5 min, 37 °C) in the absence or presence of IBMX (100 μM), cilostamide (1 μM) or rolipram (25 μM), followed by incubation (37 °C) with insulin (0.5 nM, 5 min), glimepiride (10 μM, 60 min), palmitate (1 mM, 120 min) or GO (10 mU/mL, 20 min) prior to the addition of isoproterenol (final concentration 1 μM), ADA (1 U/mL) or forskolin (25 μM) as indicated. After further incubation (2 h), the medium was separated from the adipocytes and analyzed for glycerol released. Inhibition of isoproterenol-, ADA- or forskolin-induced glycerol release in the absence of PDE inhibitor was set at 100% for insulin, glimepiride, palmitate, and GO, each. (Means ± SD, $n = 4$ adipocyte preparations with incubations in duplicate each; * indicates significant differences compared to the inhibition of isoproterenol-, ADA- or forskolin-induced glycerol release by insulin, glimepiride, palmitate and GO in the absence of inhibitor at $p < 0.01$.)

(data not shown). These findings demonstrated that the antilipolytic activity of GO action is mediated by H_2O_2. Loss of H_2O_2 by cell breakage and release of H_2O_2-degrading enzymes was determined with exogenously added H_2O_2 (see Materials and Methods) and calculated as being less than 15% under the experimental conditions used. These findings provided first evidence that in adipocytes inhibition of cAMP-induced lipolysis by glimepiride, palmitate and H_2O_2 critically depends on upregulation of cAMP degradation rather than on interference with (receptor-mediated) cAMP synthesis. The same is apparently true for the antilipolytic activity of insulin which, however, may encompass cAMP-independent mechanisms, in addition, such as the previously reported insulin-triggered dephosphorylation of HSL (*43*).

The molecular basis for the initiation of lipolysis in adipocytes is regarded to rely on the PKA-dependent phosphorylation of the major TAG and DAG lipases, ATGL and HSL, respectively, as well as of the major LD-associated protein, perilipin (*44*). Phosphorylated HSL and perilipin have been shown to translocate from the cytosol to LD and *vice versa* from LD to the cytosol, respectively, which apparently leads to increased accessibility of LD for digestion of the contained TAG by HSL (*10*, *11*). Both phosphorylation and translocation are antagonized by insulin resulting in inhibition of lipolysis. To study whether the antilipolytic activity of glimepiride, palmitate and H_2O_2 also depends on interference with HSL and perilipin translocation, isolated rat adipocytes were incubated with these agents, challenged with isoproterenol or dibutyryl-cAMP and then analyzed for the association of HSL and perilipin with LD. Isoproterenol or dibutyryl-cAMP increased the amount of LD-associated HSL by 6- to 7-fold and decreased that of perilipin-A by 90% compared to the basal state (Figure 2). The isoproterenol-induced translocation of HSL to and of perilipin-A from LD was reduced significantly by maximally effective concentrations of insulin, glimepiride, palmitate and GO. In contrast, the dibutyryl-cAMP-induced translocation of HSL and perilipin-A remained unaffected by glimepiride, palmitate and GO, and was moderately but significantly diminished by insulin, only (Figure 2). The significant reduction of the isoproterenol-induced perilipin-A translocation by GO was not paralleled to a corresponding decrease in HSL translocation which might explain the observed failure of GO to counteract the dibutyryl-cAMP-induced lipolysis (see Figure 1).

Upon incubation of the adipocytes with isoproterenol or dibutyryl-cAMP for 2 h, the period routinely used for assaying lipolysis inhibition, the amounts of the neutral lipids (TAG, cholesteryl ester, unknown lipid species) found associated with LD tended to decrease but remained almost unaltered during the concomitant presence of insulin (Table 1). Palmitate, glimepiride or GO treatment reversed the isoproterenol- but not the dibutyryl-cAMP-induced reductions in the neutral lipids. However, all these changes were only trends which did not reach statistical significance. Remarkably, there were no trends for changes in the amounts of LD-associated phospholipids, cholesterol and DAG upon challenge with isoproterenol alone or in combination with insulin, palmitate, glimepiride or GO within the assay period and detection limit (Table 1). Prolonged periods of isoproterenol stimulation (18−30 h) in the absence but not presence of the four antilipolytic agents led to significant reductions in the amounts of neutral lipids, cholesterol, and phospholipids (data not shown). These findings argue for a general blockade by insulin, glimepiride, palmitate and H_2O_2 of the apparently coordinated lipolytic degradation of neutral lipids and phospholipids at LD rather than for selective stabilization or upregulation of the LD surface phospholipid monolayer, which is assumed to act as barrier for HSL and ATGL. Immunoblotting for typical LD-associated proteins demonstrated comparable amounts of perilipin-A, ADRP, TIP47, caveolin-1 and vimentin (*45*−*47*) in the top fraction of LD

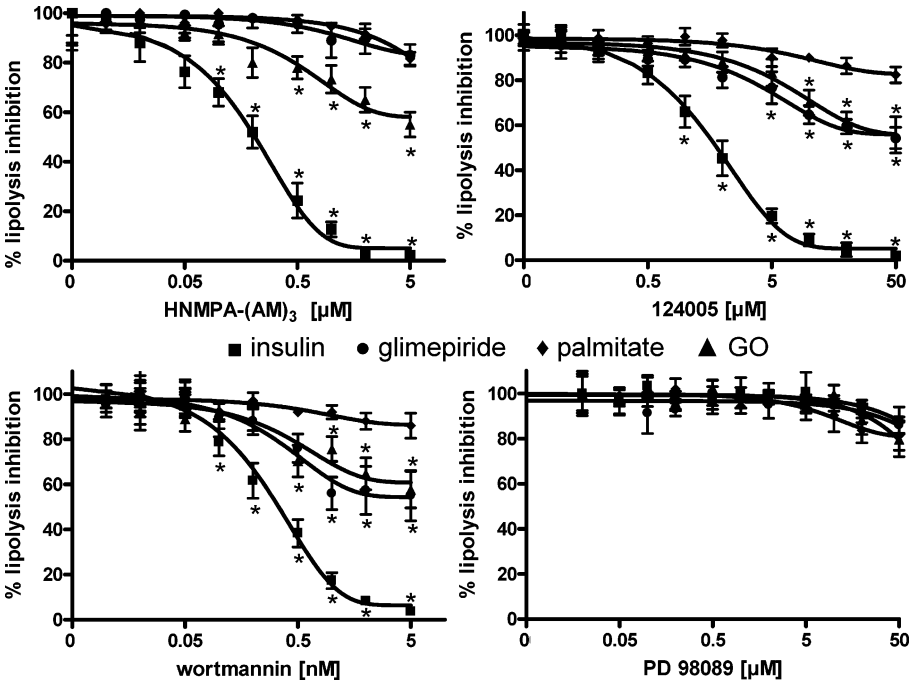

FIGURE 5: Effect of the inhibition of IR, PI3′K, PKB and MAPKK on the blockade of the isoproterenol-stimulated release of glycerol by insulin, glimepiride, palmitate and GO. Isolated rat adipocytes were incubated (5 min, 37 °C) in the absence or presence of increasing concentrations of HNMPA-$(AM)_3$, wortmannin, 124005 or PD098059 prior to the addition of insulin (final concentration 0.5 nM, 5 min), glimepiride (10 μM, 60 min), palmitate (1 mM, 120 min) or GO (10 mU/mL, 20 min) as indicated. After further incubation (15 min), isoproterenol (final concentration 1 μM) was added and the incubation continued. After 2 h the medium was separated from the adipocytes and analyzed for glycerol released. Inhibition of glycerol release in the absence of inhibitor was set at 100% for insulin, glimepiride, palmitate, and GO, each. (Means ± SD, $n = 3$ adipocyte preparations with incubations in quadruplicate each; * indicates significant differences compared to the inhibition of isoproterenol-induced lipolysis by insulin, glimepiride, palmitate and GO in the absence of inhibitor at $p < 0.01$.)

from untreated and palmitate-, glimepiride- or GO-treated adipocytes (Figure 3). The considerable abundance of perilipin-A compared to ADRP and TIP47 is in agreement with the reported predominant expression of this PAT protein at LD of mature primary adipocytes (*34*, *48*). Thus, lipolysis inhibition by palmitate, glimepiride and H_2O_2 relies on the specific blockade of the cAMP-dependent translocation of HSL and perilipin to and from LD, respectively.

Different PDE Isoforms Mediate Inhibition of Lipolysis by Insulin, H_2O_2, Palmitate and Glimepiride. Inhibition of cAMP-dependent translocation of HSL and perilipin by insulin in adipocytes is based mainly on the degradation of cAMP by PDE3B, and to a minor degree PDE4. To study whether the antilipolytic activities of glimepiride, palmitate and H_2O_2 also depend on PDE activity, isolated rat adipocytes were incubated with these stimuli in the presence of the cell-permeable unspecific PDE inhibitor IBMX, the PDE3B inhibitor cilostamide, or the PDE4 inhibitor rolipram and after lipolytic challenge assayed for lipolysis (Figure 4). IBMX reduced inhibition of the isoproterenol-, ADA- and forkolin-induced lipolysis by glimepiride, palmitate, GO and insulin by 75−90%. Cilostamide blocked lipolysis inhibition by insulin by 40−50%, but did not affect significantly the antilipolytic effect of glimepiride, palmitate and GO. In contrast, rolipram diminished lipolysis inhibition by glimepiride, palmitate and GO by 70−85%, but by insulin nonsignificantly by 20−25%, only. Rolipram and cilostamide in combination antagonized lipolysis inhibition by all four agents and even more efficiently than IBMX. Thus, down-regulation of cAMP-induced lipolysis by insulin, glimepiride, palmitate and H_2O_2 in rat adipocytes critically depends on PDE activity. The PDEs engaged, however, differ between insulin (predominantly cilostamide-sensitive) and glimepiride, palmitate or H_2O_2 (rolipram-sensitive).

Upregulation of the PDE activity by insulin in adipocytes has been demonstrated to depend on the activation of PI3′K and PKB, two key components downstream of the IR, rather than on activation of the MAPK(K) acting downstream of PI3′K and PKB. To study whether lipolysis inhibition by glimepiride, palmitate and H_2O_2, which apparently also relies on PDE activity, engages (parts of the) insulin signaling, isolated rat adipocytes were incubated with these agents in the presence of increasing concentrations of the IR kinase inhibitor HNMPA-$(AM)_3$, the PI3′K inhibitor wortmannin, the PKB inhibitor 124005 or the MAPKK inhibitor PD98089 and then assayed for isoproterenol-induced lipolysis (Figure 5). Blockade of isoproterenol-induced lipolysis by insulin and GO was significantly and concentration-dependently reduced by HNMPA-$(AM)_3$, wortmannin and 124005 to almost basal values and by up to 30−40%, respectively. In contrast, blockade of lipolysis by glimepiride was reduced by wortmannin and 124005 significantly by up to 40%, only, but not affected by HNMPA-$(AM)_3$. Lipolysis inhibition by palmitate was not altered significantly by these three inhibitors of insulin signaling. Thus, the antilipolytic activity of glimepiride and H_2O_2, but not palmitate, depends on up-regulation of insulin signaling at the level of the PI3′K/PKB and IR/PI3′K/PKB, respectively, albeit to a moderate degree only. PD98089 had no significant effect demonstrating that the MAPK cascade is not involved in lipolysis inhibition by palmitate, H_2O_2 and glimepiride as also shown previously for insulin (*14*).

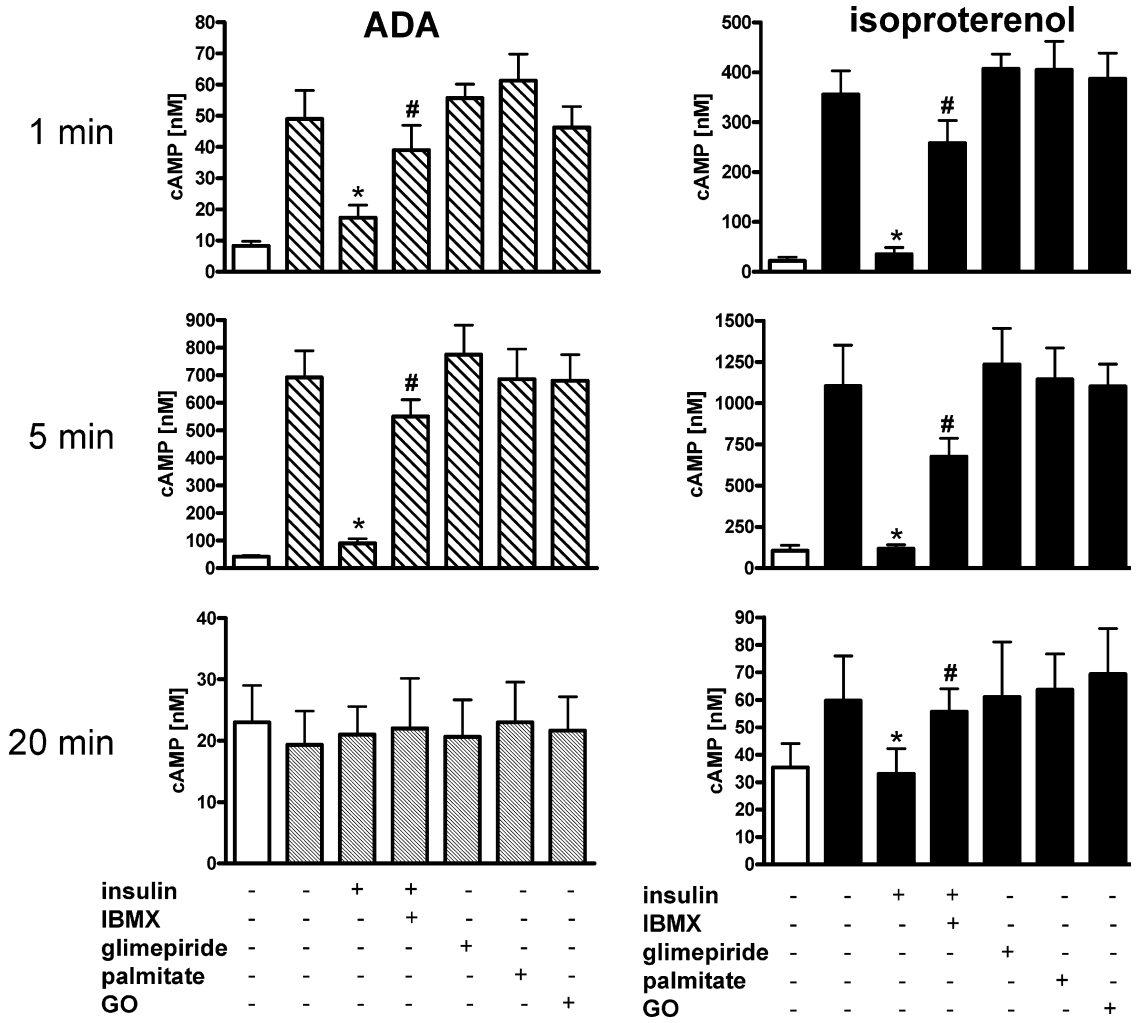

FIGURE 6: Effect of insulin, glimepiride, palmitate and GO on cytosolic cAMP level. Isolated rat adipocytes were incubated (5 min, 37 °C) without or with IBMX (100 μM) and then treated (37 °C) in the absence or presence of insulin (0.5 nM, 5 min), glimepiride (10 μM, 60 min), palmitate (1 mM, 120 min) or GO (10 mU/mL, 20 min) prior to the addition of isoproterenol (final concentration 1 μM, filled bars) or ADA (1 U/mL, hatched bars) or buffer alone (open bars). After further incubation (1, 5 or 20 min), the adipocytes were separated from the medium. Cytosol was prepared in the presence of IBMX (100 μM) and analyzed for cAMP levels. (Means ± SD, $n = 3$ adipocyte preparations with incubations in triplicate each; */# indicate significant differences compared to the isoproterenol- or ADA-induced cAMP levels in the absence of insulin, glimepiride, palmitate, GO and IBMX at $p < 0.01$ [*] or presence of insulin at $p < 0.05$ [#].)

Palmitate, Glimepiride and H_2O_2 Induce Upregulation of PDE and 5′-Nuc Activities at LD. The activation of PDE3B in adipocytes in response to insulin triggers a pronounced decline in cytosolic cAMP levels effective during the short period of insulin receptor-dependent PI3′K and PKB activation. To study whether challenge with glimepiride, palmitate and H_2O_2 leads to decreases in cytosolic cAMP, isolated rat adipocytes were incubated with these agents prior to challenge with ADA and isoproterenol for various periods. Determination of the cAMP levels in the cytosol revealed (Figure 6) ADA- (left panels) or isoproterenol- (right panels) induced drastic increases at 1 and 5 min, but not at 20 min, and thus confirmed the short-lived nature of the cAMP signal, which is sufficient for the initiation of lipolysis. Insulin significantly lowered the isoproterenol- and ADA-induced cAMP levels to almost basal levels in the absence but not presence of IBMX. In contrast, glimepiride, palmitate and GO did not exert significant effects on the elevated cytosolic cAMP levels at all time points studied (Figure 6). Thus, the antilipolytic activity of glimepiride, palmitate and H_2O_2 does not depend on the lowering of total cytosolic cAMP to a degree as elicited by insulin and detectable with the assay method used.

The apparently constant total cytosolic cAMP levels during lipolysis inhibition by glimepiride, palmitate and H_2O_2 are surprising on the basis of the observed requirement of PDE action. This may be explained by compartmentalization of the cAMP degradation since local reductions in cAMP in the immediate vicinity of the LD could prevent the cAMP-dependent translocation of HSL and perilipin but may escape detection by measurement of total cytosolic cAMP levels. The local degradation of cAMP may be catalyzed by (so far unknown) PDEs and/or other activities which become expressed at LD in response to glimepiride, palmitate and H_2O_2. To test for this possibility, LD and microsomes were prepared from isolated rat adipocytes treated with these agents prior to challenge with isoproterenol and then assayed for the conversion of exogenous cAMP to adenosine in the absence or presence of various inhibitors (Figure 7).

The rate of conversion of cAMP to adenosine was significantly higher with LD from glimepiride-, palmitate- and GO-treated adipocytes compared to those from basal

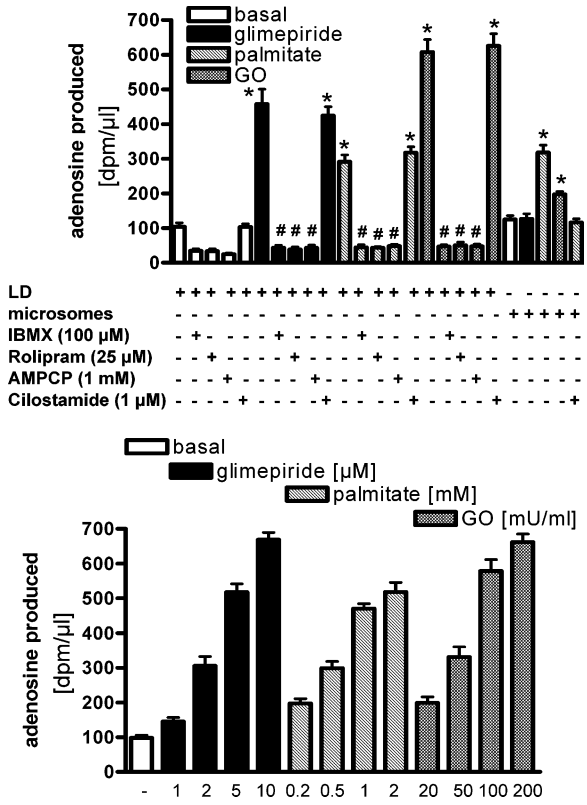

FIGURE 7: Effect of glimepiride, palmitate and GO on the conversion of cAMP to adenosine by LD. Isolated rat adipocytes were incubated (37 °C) in the absence (basal) or presence of glimepiride (10 μM, 60 min), palmitate (1 mM, 120 min) or GO (10 mU/mL, 20 min) (upper panel), or increasing concentrations of glimepiride, palmitate and GO (lower panel) and then separated from the medium. LD (both panels) and microsomes (upper panel) were prepared from the adipocytes and then assayed for the conversion of cAMP into adenosine in the absence (lower panel) or presence (upper panel) of inhibitors as indicated. (Means ± SD of 4 adipocyte preparations with incubations in duplicate each; */# indicates significant differences compared to the basal [*] or glimepiride-/palmitate-/GO-induced [#] adenosine production in the absence of inhibitor at $p < 0.01$.)

cells (Figure 7, upper panel). The EC_{50}-values closely corresponded to the IC_{50}-values for lipolysis inhibition by each agent (Figure 7, lower panel, see Figure 1). The involvement of PDE and 5′-Nuc activities in the conversion of cAMP to adenosine by the LD was demonstrated by its significant lowering in the presence of IBMX and rolipram (but not cilostamide), as well as the 5′-Nuc inhibitor AMPCP (Figure 7, upper panel). The stability of the interaction of the cAMP-to-adenosine converting enzyme(s) with LD was demonstrated by recentrifugation on sucrose gradients with recovery of the major portion of the loaded conversion activity from the top fraction together with the LD. Conversion of cAMP to adenosine was also significantly increased (in cilostamide-sensitive fashion) with microsomes from palmitate- and GO-treated, but not glimepiride-treated adipocytes (Figure 7, upper panel). The addition of exogenous 5′-Nuc to the conversion assay did not significantly increase the rate of adenosine production (data not shown). This argues against AMP-to-adenosine cleavage by 5′-Nuc being rate-limiting for the overall cAMP-to-adenosine conversion by isolated LD. Taken together, glimepiride, palmitate and H_2O_2 induce the upregulation of a rolipram-sensitive PDE and a AMPCP-sensitive 5′-Nuc at LD.

Characterization of the LD-Associated PDE and 5′-Nuc. The nature of the LD-assocated PDE activity in rat adipocytes was further characterized by studying its sensitivity toward isoform-specific PDE inhibitors at concentrations which exceed their IC_{50}-values by about 10-fold (Table 2). As expected, microsomal cAMP-to-adenosine conversion was sensitive toward cilostamide and, to a lower but significant degree, rolipram and cGMP, which is compatible with PDE3B and PDE4 representing the major PDE isoforms at the endoplasmic reticulum of rat adipocytes. cAMP-to-adenosine conversion by LD was completely blocked by IBMX, the nonhydrolyzable cAMP-analogue, SP-8-Br-cAMPS and rolipram, whereas downregulation by isoform-specific inhibitors of PDE1 (200 μM vinpocetine), 2 (0.1 μM BAY 60-7550), 3 (1 μM cilostamide), 5 (0.1 μM sildenafil), 6 (5 μM zaprinast), 7 (BRL 50481), 8 (10 μM dipyridamole), 9 (5 μM zaprinast) and 10 (10 μM dipyridamole) had no significant effect. The same was true for excess of cGMP, which argues for cAMP specificity of the relevant LD-associated PDE and its nonidentity with the cGMP-inhibitable PDE3B as well as cGMP/cAMP-specific PDE5, 6, 9, 10 and 11. Thus, the LD-associated PDE of rat adipocytes is apparently not identical with the PDE isoforms 1−3, 5−11. It may be related to PDE4 or constitute a novel type of PDE.

To test for these possibilities, proteins were extracted from LD, which had been treated with GO, and then immunoblotted for distinct PDE isoforms, in particular, PDE4, in comparison with microsomes, cytosol and DIGs (Figure 8). In agreement with recent reports cytosol of rat adipocytes contained PDE4A, PDE4B, PDE4C and PDE4D, exclusively (*49*), microsomes PDE3A and predominantly PDE3B (*15*, *50*) as well as PDE8, and DIGs PDE3B and PDE4C. In LD low amounts of PDE7, PDE3B, PDE2 and PDE8 (declining order of signal strength) were only detectable. This PDE distribution was not altered with insulin-, glimepiride-, palmitate-treated or untreated adipocytes (data not shown). However, these immunoblotting data allowed semiquantitative evalution of PDE expression, only, due to the unknown reactivity of the isoform-specific antibodies used and the lack of the corresponding purified rat PDE isoforms as appropriate loading and normalization controls. For further substantiation of the nonidentity of the LD-associated PDE, which is upregulated by the lipolytic agents, with PDE7, PDE3B and PDE2, their extraction behavior from LD of GO-treated adipocytes was compared to that of the cAMP-to-adenosine conversion activity (Figure 9). Treatment with high salt but not bacterial PI-PLC led to release of significant portions of PDE3B (95%), PDE7 (70%) and PDE2 (97%) from the LD into the infranatant upon sucrose gradient centrifugation compared to control incubations (upper panels). In contrast, the LD-associated cAMP-to-adenosine conversion activity was almost unaffected by high salt treatment compared to control but significantly released from the LD by PI-PLC by almost 75% (lower panel). This suggests peripheral association of PDE3B, PDE7 and PDE2 with the LD *via* salt bridges whereas the (PDE component of the) cAMP-degrading activity seems to interact more tightly with the LD TAG core and/or phospholipid monolayer. Its apparent release by lipolytic cleavage hints to a role of these phospholipids for its interaction with the LD surface and/or to an anchoring function of a putative phospholipid structure,

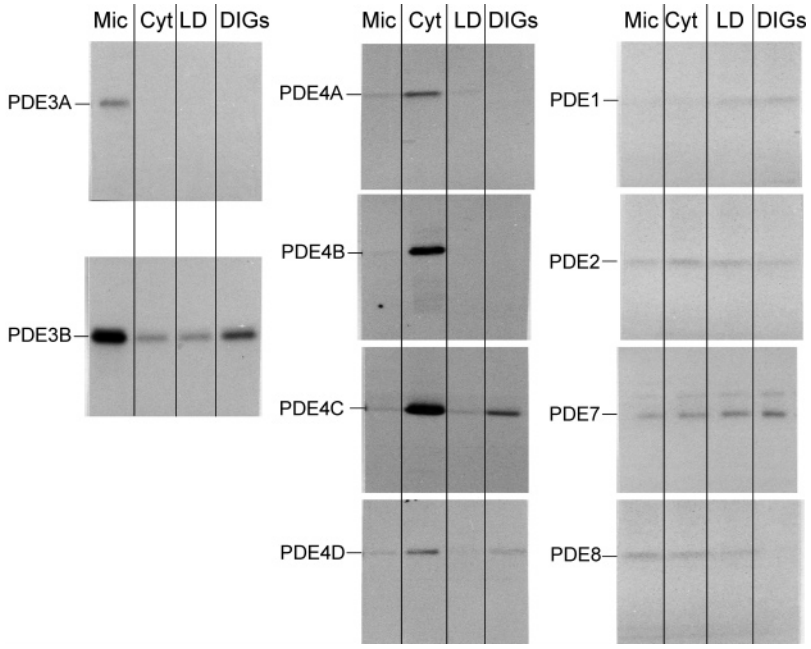

FIGURE 8: Subcellular distribution of PDE isoforms. LD, microsomes (Mic), DIGs and cytosol (Cyt) were prepared from isolated rat adipocytes which had been incubated (37 °C) in the presence of GO (100 mU/mL, 20 min) as described in Materials and Methods. Proteins extracted from LD and precipitated under denaturing conditions, microsomes, DIGs and cytosol (50−100 μg) were subjected to SDS−PAGE and immunoblotted for PDE isoforms. Lumiimages of a typical experiment are shown repeated once with similar results.

Table 2: Effect of PDE Inhibitors on the Conversion of cAMP to Adenosine by LD and Microsomes[a]

			LD			microsomes		
PDE inhibitor	PDE affected	conc [μM]	glimepiride	palmitate	GO	glimepiride	palmitate	GO
no			100 ± 9	100 ± 13	100 ± 8	100 ± 6	100 ± 9	100 ± 6
cilostamide	3	1	88 ± 9	79 ± 7	85 ± 9	**15 ± 3**	**17 ± 4**	**13 ± 2**
rolipram	4	25	**9 ± 4**	**12 ± 3**	**7 ± 2**	**72 ± 10**	**66 ± 13**	**77 ± 10**
cGMP	3,5,6, 9−11	100	88 ± 4	78 ± 6	90 ± 8	**43 ± 12**	**56 ± 13**	**48 ± 8**
IBMX	1−11	10	**3 ± 1**	**3 ± 3**	**5 ± 3**	**5 ± 1**	**6 ± 2**	**8 ± 2**

[a] Isolated rat adipocytes were incubated (37 °C) in the presence of glimepiride (10 μM, 60 min), palmitate (1 mM, 120 min) or GO (10 mU/mL, 20 min) and then separated from the medium for the preparation of LD and microsomes. LD and microsomes were incubated (5 min, 37 °C) in the absence or presence of various PDE inhibitors at the concentrations indicated and then assayed for cAMP-to-adenosine conversion as described in Materials and Methods. The activity measured with LD or microsomes in the absence of inhibitor was set at 100% for glimepiride, palmitate and GO, each. (Means ± SD, $n = 4$ adipocyte preparations with determinations in triplicate; bold numbers indicate significant differences compared to the absence of PDE inhibitor at $p < 0.05$.)

such as glycosylphosphatidylinositol, covalently attached to the protein moiety (*51*). The different extraction characteristics of the cAMP-to-adenosine conversion activity on one side and of the PDE3B, PDE7 and PDE2 on the other side together with the rather low expression of the latter strongly argues for noninvolvement of the known adipocyte PDE isoforms in cAMP degradation by LD in palmitate-, glimepiride- and GO-treated rat adipocytes.

DISCUSSION

Since its discovery 50 years ago, cAMP has been the prototypical second messenger, translating the actions of numerous extracellular effectors into consequences for virtually every aspect of cellular function. Among other signaling paradigms that were first developed from cAMP was the issue of compartmentalization: the concept whereby cAMP can be partitioned to discrete regions of the cell with numerous regulatory consequences (*52*). However, whereas meanwhile some of the mechanisms underlying the spatiotemporal manifestation of compartmentalization of cAMP synthesis at the level of G-protein-coupled receptors, PKA, A-kinase-anchoring proteins and adenylyl cyclases have been unraveled (*26*, *53*, *54*), little is known so far about how PDEs, central elements for the control of cAMP degradation, participate in higher-order signaling complexes and contribute to cAMP compartmentalization (*25*, *55*, *56*). Recent studies proposed that distinct PDE isoforms regulate different cAMP pools in cardiomyocytes (*57*) and adipocytes (*58*). PDEs belong to a complex and diverse superfamily of at least 11 structurally related, highly regulated, and functionally distinct gene families (PDE1−PDE11) (*59*, *60*). The PDE3B isoform is abundant in cells of importance for energy homeostasis including hepatocytes, brown and white adipocytes, and pancreatic β-cells (*15*, *61*). In adipocytes, activation of PDE3B is thought to be the major mechanism whereby insulin lowers total cAMP levels in the cytosol and thereby antagonizes cAMP-mediated lipolysis.

The present study strongly suggests that local degradation of cAMP in the vicinity of LD by the LD-associated cAMP-to-adenosine conversion activity represents an additional antilipolytic mechanism in rat adipocytes that is used by three completely different agents, palmitate, the antidiabetic sulfonylurea drug glimepiride, and H_2O_2 (Figure 10). This

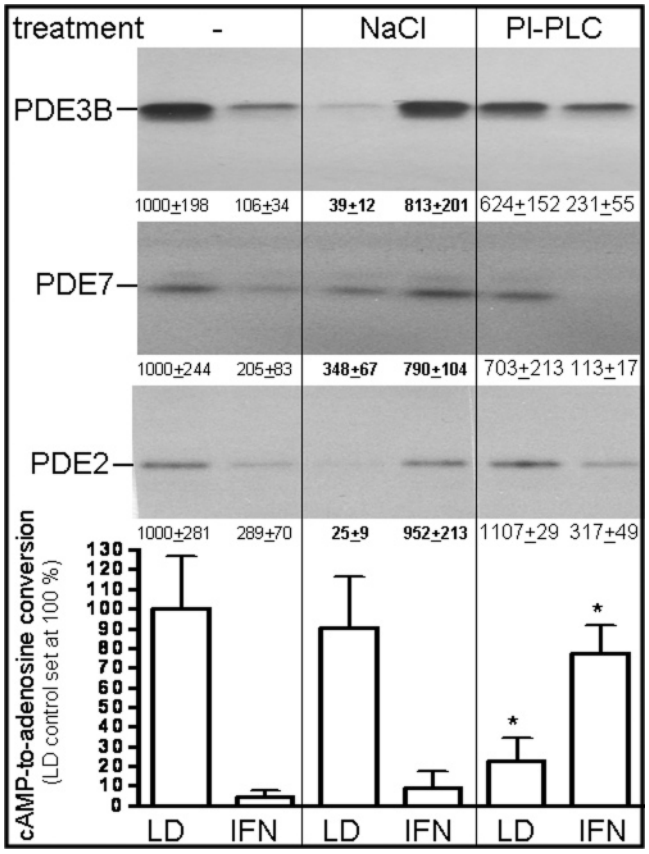

FIGURE 9: Release of PDE isoforms and cAMP-to-adenosine conversion activity from LD. Isolated rat adipocytes were incubated (37 °C) in the presence of GO (100 mU/mL, 20 min) and then separated from the medium. LD were prepared from the adipocytes and then left untreated or treated with 1.5 M NaCl (1 h, 37 °C) or with PI-PLC (*B. cereus*, 1 U/mL, 2 h 30 °C, 0.1% TX-100). Thereafter, the incubation mixtures were subjected to sucrose gradient centrifugation as described in Materials and Methods. LD were removed from the top fraction and extracted for proteins under native conditions. Proteins released were removed from the infranatant (IFN) by suction. Proteins were precipitated under native conditions and after dissolution immunoblotted for PDE isoforms (upper panels) or assayed for the conversion of cAMP into adenosine (lower panel) with the amount of protein or conversion activity determined for untreated LD set at 1000 arbitrary units or 100%, respectively. (Means ± SD, $n = 3$ adipocyte preparations with treatments in triplicate each; bold numbers and * indicate significant differences compared to the PDE amounts and cAMP-to-adenosine conversion of LD and IFN from untreated LD at $p < 0.01$.)

conclusion is based on the following experimental evidence: (i) The three agents block lipolysis (Figure 1), reduce the amount of LD-associated HSL and increase the amount of LD-associated perilipin which are raised and lowered, respectively, in response to cAMP-elevation by isoproterenol, ADA, forskolin, but not in response to nonhydrolyzable dibutyryl-cAMP (Figure 2). (ii) Lipolysis inhibition by the three agents is blocked by the general PDE inhibitor, IBMX, and the PDE4 inhibitor, rolipram, but not by the PDE3 inhibitor, cilostamide, which abrogates completely the antilipolytic activity of insulin (Figure 4, Table 2). (iii) Inhibition of insulin signaling reduces the antilipolytic activity of the three agents by less than 50% (H_2O_2, glimepiride) or not at all (palmitate) (Figure 5). These findings argue for involvement of cAMP degradation and rolipram-sensitive PDE action for the major portion of their antilipolytic activity which do not encompass insulin signaling and PDE3B. In addition, a minor portion of the lipolysis inhibition by H_2O_2 and glimepiride apparently requires activation of the IR and/or downstream signaling, respectively, which presumably relies on the known inhibition of IR dephosphorylation by H_2O_2 (*19*, *20*) and known stimulation of IR-independent tyrosine phosphorylation of the insulin receptor substrate-1 by glimepiride (*29*, *39*). (iv) The relative lipid composition of LD does not change upon challenge with the antilipolytic agents (Table 1) arguing against impaired accessibility of the LD TAG core for lipases by stabilization of the LD surface phospholipid monolayer. (v) The antilipoytic agents do not exert significant alterations in total cytosolic cAMP (Figure 6) arguing for involvement of cAMP compartmentalization. (vi) LD from glimepiride-, palmitate- and H_2O_2-induced adipocytes, but not from basal and insulin-induced cells, harbor a rolipram-sensitive cilostamide-insensitive cAMP-to-adenosine conversion activity (Figure 7). This activity most likely does not rely on the PDE isoforms 1, 2, 3A, 3B, 4A, 4B, 4C, 4D, 7 and 8 based on (i) their low expression at LD compared to that at microsomes (PDE3A, PDE3B, PDE8) and cytosol (PDE4A, PDE4B, PDE4C, PDE4D, PDE8) of H_2O_2-induced adipocytes (Figure 8), (ii) the failure of inhibitors of PDE1, 2, 3, 7 and 8 to suppress palmitate-, glimepiride- and H_2O_2-induced cAMP-to-adenosine conversion (Table 2 and Results section) and (iii) the extraction behavior of PDE3B, 7 and 2, the predominant LD-associated PDE isoforms of rat adipocytes, which differs from that of the LD-associated cAMP-to-adenosine conversion activity (Figure 9).

Previous analysis of the presence of PDE4 in untreated rat adipocytes by PCR revealed mRNA expression of all four isoforms (*49*) in agreement with our immunoblotting data (Figure 8). Furthermore, it was shown that PDE4 contributes to 10−20% of total PDE activity in defatted adipocyte homogenates according to its rolipram sensitivity with about equal distribution between particulate and cytosolic fractions (*50*). Future studies on the distribution and function of PDEs, in general, and rolipram-sensitive PDE, in particular, in adipocytes have to consider LD as putative compartment and the LD-associated cAMP-to-adenosine conversion activity as putative PDE for cAMP degradation. So far, LD have been considered as TAG storage containers, only, formed by special structural and coat proteins, which transiently harbor enzymes for TAG synthesis (e.g., glycerol-3-phosphate acyltransferase; see ref *62*) and degradation (e.g., hormone-sensitive lipase; see refs *36* and *63*). The present findings will broaden this view in that enzymes regulating TAG metabolism *via* modulation of the cAMP levels in the immediate vicinity of the sites of TAG synthesis and degradation apparently can be regarded as transiently LD-associated proteins under certain (antilipolytic) states of the adipocytes (Figure 10). Moreover, the inhibition of the cAMP-to-adenosine conversion activity by rolipram formerly regarded as being specific for PDE4 (*64*) necessitates additional studies about the roles of the apparently novel PDE component and PDE4 in adipocyte lipolysis on basis of more specific inhibition at the level of activity or expression.

The apparently high concentrations of glimepiride and FA used as antilipolytic stimuli in the present study raise the question about their physiological relevance. The serum peak levels of total (free and albumin-bound) glimepiride and FA during therapy of type II diabetes patients and starvation of

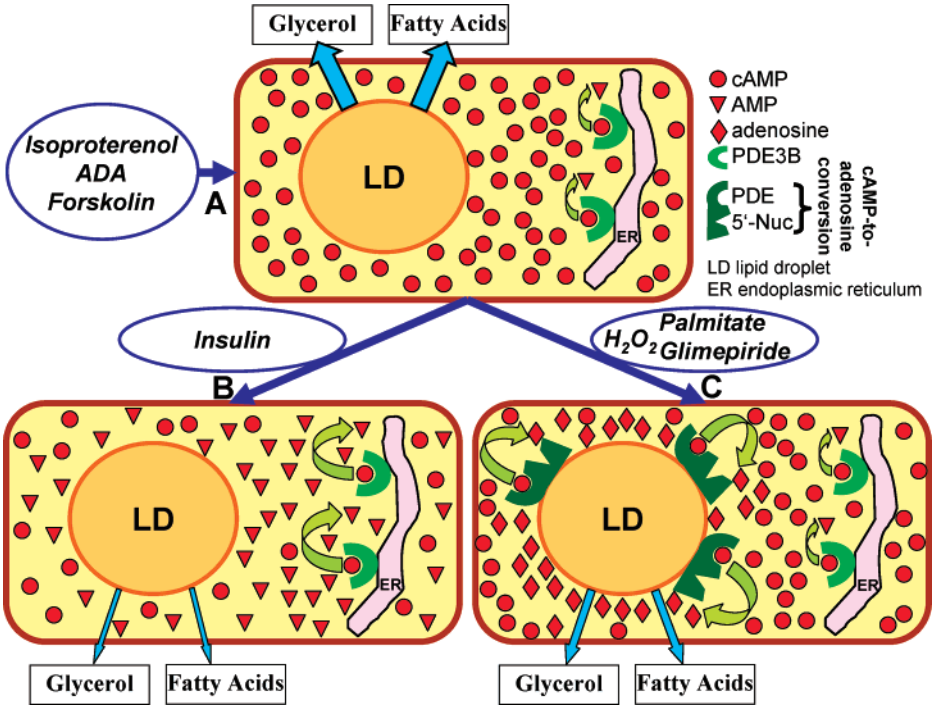

FIGURE 10: Model for the inhibition of the isoproterenol-, ADA- and forskolin-induced lipolysis by palmitate, glimepiride and H_2O_2 in rat adipocytes. (A) Short-term challenge with isoproterenol, ADA or forskolin leads to elevation of total cytosolic cAMP. This results in the release of glycerol and fatty acids in the course of cAMP-dependent phosphorylation and translocation of HSL to and perilipin from the LD (not shown, see text). cAMP degradation by microsomal PDE3B is low. (B) Insulin causes degradation and thereby lowering of total cytosolic cAMP through activation of microsomal PDE3B. This results in drastically diminished glycerol and fatty acid release in the course of dephosphorylation and translocation of HSL from and perilipin to LD (not shown). (C) Palmitate, glimepiride and H_2O_2 cause degradation and thereby lowering of cAMP in the immediate vicinity of the LD, only, through upregulation of the cAMP-to-adenosine conversion activity, which is presumably constituted by distinct PDE and 5′-Nuc enzymes, at the surface of the LD. This results in partially abrogated glycerol and fatty acid release in the course of dephosphorylation and translocation of HSL from and perilipin to LD (not shown). cAMP degradation by microsomal PDE3B is low and total cytosolic cAMP remains elevated.

rodents or humans, respectively, approach up to 1 μM (*8*) and 1 mM, respectively. They are thus within the range of total glimepiride and palmitate concentrations present in the incubation medium (which contained BSA) and shown here to be effective in antilipolysis and upregulation of the cAMP-to-adenosine conversion activity at LD in isolated rat adipocytes. During maximal lipolysis the intracellular FA levels have been reported to be much higher (40−60 mM; see ref *5*) and may exceed the binding capacity of cytosolic FA-binding proteins resulting in increased levels of free FA. Under these conditions, feedback inhibition is assumed to restrict further lipolysis which may be based on one or several of the following mechanisms: (i) Reduction in cytosolic ATP by the upregulated lipolytic phosphorylation cascade (*21*) or inhibition of oxidative phosphorylation or increase in ionic permeability of mitochondria, which both have been attributed to nonspecific association of FA with mitochondrial membranes (*22*), or increased formation of cAMP from ATP, (ii) direct inhibitory effect of FA and long-chain acyl-CoA on lipases by product inhibition (*65*, *66*) and (iii) increase in reactive oxygen species with insulin-mimetic antilipolytic activity in course of upregulated mitochondrial FA oxidation (*3*, *4*). However, the observed blockade of the lipolysis inhibition by palmitate- (and glimepiride and H_2O_2) (Figure 4) as well as cAMP-to-adenosine conversion by LD (Figure 7) in the presence of PDE inhibitors makes operation of these putative antilipolytic feedback mechanisms in rat adipocytes under the experimental setup used unlikely. PDE inhibition should not lead to normalization of ATP or intracellular FA/acyl-CoA levels or antagonize detrimental effects of FA or reactive oxygen species. Moreover, the well-known blockade of lipolysis by inhibitors of oxidative phosphorylation (antimycin A, rotenone) or ATP synthesis (oligomycin) (*21*, *22*) was not abrogated by IBMX (data not shown). This confirms that the antilipolytic activity of palmitate (and glimepiride, H_2O_2) relies on specific PDE inhibition rather than ATP depletion.

Interestingly, analysis of the cAMP metabolism in the lower eukaryote *Dictyostelium discoideum* revealed a function of the 7 PDE isoforms (*67*) different from cAMP compartmentalization. *Dictyostelium discoideum* cells contain intracellular and extracellular pools of cAMP which are regulated by combinations of two distinct PDEs, each having different kinetic properties. One PDE has high affinity for cAMP and relatively low capacity, while the opposite is true for the other PDE. It was shown that these properties in combination allow the degradation of cAMP with approximately first-order kinetics over a wide range of concentrations which actually occur *in vivo* during multicellular development and chemotactic response of *Dictyostelium discoideum*. In analogy, it is conceivable that in adipocytes the combination of the LD-associated PDE and other PDEs, such as PDE3B and PDE4, which both have been identified at the cytoplasmic faces of plasma membranes and endoplasmic reticulum membranes (*24*, *26*, *68*, *69*), is tuned in such a way that the control of the cytosolic cAMP pool is guaranteed over a wide concentration range during inhibition of lipolysis. It would be interesting to study whether the catalytic

properties of the PDE component of the cAMP-to-adenosine conversion activity complement those of its putative counterpart(s).

REFERENCES

1. Frayn, K. N. (2002) Adipose tissue as a buffer for daily lipid flux, *Diabetologia 45*, 1201−1210.
2. Langin, D. (2006) Adipose tissue lipolysis as a metabolic pathway to define pharmacological strategies against obesity and the metabolic syndrome, *Pharmacol. Res. 53*, 482−491.
3. Little, S. A., and de Haen, C. (1980) Effects of hydrogen peroxide on basal and hormone-stimulated lipolysis in perifused rat fat cells in relation to the mechanism of action of insulin, *J. Biol. Chem. 255*, 10888−10895.
4. Mukherjee, S. P. (1980) Mediation of the antilipolytic and lipogenic effects of insulin in adipocytes by intracellular accumulation of hydrogen peroxide, *Biochem. Pharmacol. 29*, 1239−1246.
5. Burns, T. W., Langley, P. E., Terry, B. E., and Robinson, G. A. (1978) The role of free fatty acids in the regulation of lipolysis by human adipose tissue cells, *Metabolism 27*, 1755−1762.
6. Müller, G., Wied, S., Wetekam, E.-M., Crecelius, A., Unkelbach, A., and Pünter, J. (1994) Stimulation of glucose utilization in 3T3 adipocytes and rat diaphragm in vitro by the sulfonylureas, glimepiride and glibenclamide, is correlated with modulations of the cAMP regulatory cascade, *Biochem. Pharmacol. 48*, 985−996.
7. Müller, G. (2000) The molecular mechanism of the insulin-mimetic/sensitizing activity of the antidiabetic sulphonylurea drug amaryl, *Mol. Med. 6*, 907−933.
8. Müller, G. (2005) The mode of action of glimepiride—beyond insulin secretion, *Curr. Med. Chem. 5*, 499−518.
9. Müller, G., and Petry, S. (2005) Triacylglycerol, Storage and Mobilization of Human, in *Encyclopedia in Biochemistry and Molecular Biology* (Meyers, A., Ed.) Vol. 14, pp 621−704, Wiley-VCH, Weinheim/Germany.
10. Egan, J. J., Greenberg, A. S., Chang, M.-K., Wek, S. A., Moos, M. C., and Londos, C. (1992) Mechanism of hormone-stimulated lipolysis in adipocytes: Translocation of hormone-sensitive lipase to the lipid storage droplet, *Proc. Natl. Acad. Sci. U.S.A. 89*, 8537−8541.
11. Sztalryd, C., Xu, G., Dorward, H., Tansey, J. T., Contreras, J. A., and Kimmel, A. R. (2003) Perilipin A is essential for the translocation of hormone-sensitive lipase during lipolytic activation, *J. Cell. Biol. 161*, 1093−1103.
12. Rahn, T., Ridderstrale, M., Tornqvist, H., Manganiello, V., Fredrikson, G., Belfrage, P., and Degerman, E. (1994) Essential role of phosphatidylinositol 3-kinase in insulin-induced activation and phosphorylation of the cGMP-inhibited cAMP phosphodiesterase in rat adipocytes, *FEBS Lett. 350*, 314−318.
13. Degerman, E., Landstrom, T. R., Wijkander, J., Holst, L. S., Ahmad, F., and Belfrage, P. (1998) Phosphorylation and activation of hormone-sensitive adipocyte phosphodiesterase Type 3B, *Methods 14*, 43−53.
14. Wijkander, J., Landstrom, T. R., Manganiello, V., Belfrage, P., and Degerman, E. (1998) Insulin-induced phosphorylation and activation of phosphodiesterase 3B in rat adipocytes, possible role for protein kinase B but not mitogen-activated protein kinase or p70 S6 kinase, *Endocrinology 139*, 219−227.
15. Shakur, Y., Holst, L. S., Landstrom, T. R., Movsesian, M., Degerman, E., and Manganiello, V. (2001) Regulation and function of the cyclic nucleotide phosphodiesterase (PDE3) gene family, *Prog. Nucleic Acid Res. Mol. Biol. 66*, 241−277.
16. Cheung, P., Yang, G., and Boden, G. (2003) Milrinone, a selective PDE3 inhibitor, stimulates lipolysis, endogenous glucose production and insulin secretion, *Metabolism 52*, 1496−1500.
17. Choi, Y. H., Park, S., Hockman, S., Zmuda-Trzebiatowska, E., Svennelid, F., and Haluzik, M. (2006) Alterations in regulation of energy homestasis in cyclic nucleotide phosphodiesterase 3B-null mice, *J. Clin. Invest. 116*, 3240−3251.
18. Rahn Landstrom, T., Mei, J., Karlsson, M., Manganiello, V., and Degerman, E. (2000) Down-regulation of cyclic-nucleotide phosphodiesterase 3B in 3T3−L1 adipocytes induced by tumour necrosis factor alpha and cAMP, *Biochem. J. 346*, 337−343.
19. Mahadev, K., Wu, X., Zilbering, A., Zhu, L., Lawrence, J. T., and Goldstein, B. J. (2001) Hydrogen peroxide generated during cellular insulin stimulation is integral to activation of the distal insulin signaling cascade in 3T3-L1 adipocytes, *J. Biol. Chem. 276*, 48662−48669.
20. Goldstein, B. J., Mahadev, K., Wu, X., Zhu, L., and Motoshima, H. (2005) Role of insulin-induced reactive oxygen species in the insulin signaling pathway, *Antioxid. Redox Signaling 7*, 1021−1031.
21. Maragno, I., Dorigo, P., and Fassina, G. (1971) Effect of antimycin A on hormone-stimulated lipolysis in vitro, *Biochem. Pharmacol. 20*, 2149−2154.
22. Vallano, M. L., Lee, M. Y., and Sonenberg, M. (1983) Hormones modulate adipocyte membrane potential, ATP and lipolysis by free fatty acids, *Am. J. Physiol. 245*, E266−E272.
23. Abrahamsen, H., Baillie, G., Ngai, J., Vang, T., Nika, K., Ruppelt, A., Mustelin, T., Zaccolo, M., Houslay, M., and Tasken, K. (2004) TCR- and CD28-mediated recruitment of phosphodiesterase 4 to lipid rafts potentiates TCR signalling, *J. Immunol. 173*, 4847−4858.
24. Zhang, X., and Carey, G. B. (2004) Plasma membrane-bound cyclic AMP phosphodiesterase activity in 3T3−L1 adipocytes, *Comp. Biochem. Physiol., Part B: Biochem. Mol. Biol. 137*, 309−316.
25. Baillie, G. S., and Houslay, M. D. (2005) Arrestin times for compartmentalised cAMP signalling and phosphodiesterase-4 enzymes, *Curr. Opin. Cell. Biol. 17*, 129−134.
26. Willoughby, D. (2006) An anchored PKA and PDE4 complex regulates subplasmalemmal cAMP dynamics, *EMBO J. 25*, 2051−2061.
27. Müller, G., Hanekop, N., Kramer, W., Bandlow, W., and Frick, W. (2002) Interaction of phosphoinositolglycan(-peptides) with plasma membrane lipid rafts of rat adipocytes, *Arch. Biochem. Biophys. 408*, 17−32.
28. Müller, G., Hanekop, N., Wied, S., and Frick, W. (2002) Cholesterol depletion blocks redistribution of lipid raft components and insulin-mimetic signaling by glimepiride and phosphoinositolglycans in rat adipocytes, *Mol. Med. 8*, 120−136.
29. Müller, G., Schulz, A., Wied, S., and Frick, W. (2005) Regulation of lipid raft proteins by glimepiride- and insulin-induced glycosylphosphatidylinositol-specific phospholipase C in rat adipocytes, *Biochem. Pharmacol. 69*, 761−780.
30. Müller, G., Wetekam, E.-M., Jung, C., and Bandlow, W. (1994) Membrane association of lipoprotein lipase and a cAMP-binding ectoprotein in rat adipocytes, *Biochemistry 33*, 12149−12159.
31. Müller, G., and Wied, S. (1993) The sulfonylurea drug, glimepiride, stimulates glucose transport, glucose transporter translocation, and dephosphorylation in insulin-resistant rat adipocytes in vitro, *Diabetes 42*, 1852−1867.
32. Ngo, T. T., and Lenhoff, M. M. (1980) Assay for peroxidase and peroxidase-coupled reactions, *Anal. Biochem. 105*, 389−397.
33. Greenberg, A. S., Egan, J. J., Wek, S. A., Garty, N. B., Blanchette-Mackie, E. J., and Londos, C. (1991) Perilipin, a major hormonally regulated adipocyte-specific phosphoprotein associated with the periphery of lipid storage droplets, *J. Biol. Chem. 266*, 11341−11346.
34. Wolins, N. E., Quaynor, B. K., Skinner, J. R., Schoenfish, M. J., Tzekov, A., and Bickel, P. E. (2005) S3-12, Adipophilin, and TIP47 package lipid in adipocytes, *J. Biol. Chem. 280*, 19146−19155.
35. Tauchi-Sato, K., Ozeki, S., Houjou, T., Taguchi, R., and Fujimoto, T. (2002) The surface of lipid droplets is a phospholipid monolayer with a unique fatty acid composition, *J. Biol. Chem. 277*, 44507−44512.
36. Bartz, R., Li, W.-H., Venables, B., Zehmer, J. K., Roth, M. R., Welti, R., Anderson, G. W., Liu, P., and Chapman, K. D. (2007) Lipidomics reveals that adiposomes store ether lipids and mediate phospholipid traffic, *J. Lipid Res. 48*, 837−847.
37. Bligh, E. G., and Dyer, W. J. (1959) A rapid method of total lipid extraction and purification, *Can. J. Biochem. Physiol. 37*, 911−917.
38. Folch, J., Lees, M., and Sloane-Stanley, G. H. (1957) A simple method for the isolation and purification of total lipids from animal tissues, *J. Biol. Chem. 226*, 497−509.
39. Müller, G., Jung, C., Wied, S., Welte, S., Jordan, H., and Frick, W. (2001) Redistribution of glycolipid raft domain components induces insulin-mimetic signaling in rat adipocytes, *Mol. Cell. Biol. 21*, 4553−4567.
40. Müller, G., Jordan, H., Jung, C., Kleine, H., and Petry, S. (2003) Analysis of lipolysis in adipocytes using a fluorescent fatty acid derivative, *Biochimie 85*, 1245−1256.

41. Vertesy, L., Beck, B., Brönstrup, M., Ehrlich, K., Kurz, M., Müller, G., Schummer, D., and Seibert, G. (2002) Cyclipostins, novel hormone-sensitive lipase inhibitors from *Streptomyces* sp. DSM 13381. II. Isolation, structure elucidation and biological properties, *J. Antibiot. 55*, 480−494.
42. Soares, A. F., Guichardant, M., Cozzone, D., Bernoud-Hubac, N., Bouzaidi-Tiali, N., Lagarde, M., and Geloen, A. (2005) Effects of oxidative stress on adiponectin secretion and lactate production in 3T3-L1 adipocytes, *Free Radical Biol. Med. 38*, 882−889.
43. Yeaman, S. J. (2003) Hormone-sensitive lipase—new roles for an old enzyme, *Biochem. J. 379*, 11−22.
44. Zechner, R., Strauss, J. G., Haemmerle, G., Lass, A., and Zimmermann, R. (2005) Lipolysis: pathway under construction, *Curr. Opin. Lipidol. 16*, 333−340.
45. Blanchette-Mackie, E. J., Dwyer, N. K., Barber, R. A., Coxey, T., Takeda, C. M., Rondinone, J. L., Theodorakis, J. L., Greenberg, A. S., and Londos, C. (1995) Perilipin is located on the surface layer of intracellular lipid droplets in adipocytes, *J. Lipid Res. 36*, 1211−1226.
46. Brasaemle, D. L., Barber, T., Wolins, N. E., Serrero, G., Blanchette-Mackie, E. J., and Londos, C. (1997) Adipose differentiation-releated protein is an ubiquitously expressed lipid storage droplet-associated protein, *J. Lipid Res. 38*, 2249−2263.
47. Londos, C., Sztalryd, C., Tansey, J. T., and Kimmel, A. R. (2005) Role of PAT proteins in lipid metabolism, *Biochimie 87*, 45−49.
48. Wolins, D. E., Brasaemle, D. L., and Bickel, P. E. (2006) A proposed model of fat packaging by exchangeable lipid droplet proteins, *FEBS Lett. 580*, 5484−5491.
49. Wang, H., and Edens, N. K. (2007) mRNA expression and antilipolytic role of phosphodiesterase 4 in rat adipocytes in vitro, *J. Lipid Res. 48*, 1099−1107.
50. Snyder, P. B., Esselstyn, J. M., Loughney, K., Wolda, S. L., and Florio, V. A. (2005) The role of cyclic nucleotide phosphodiesterases in the regulation of adipocyte lipolysis, *J. Lipid Res. 46*, 494−503.
51. Orlean, P., and Menon, A. K. (2007) Thematic review series: lipid posttranslational modifications. GPI anchoring of protein in yeast and mammalian cells, or: how we learned to stop worrying and love glycophospholipids, *J. Lipid Res. 48*, 993−1011.
52. Buxton, I. L., and Brunton, L. L. (1983) Compartments of cyclic AMP and protein kinase in mammalian cardiomyocytes, *J. Biol. Chem. 258*, 10233−10239.
53. Cooper, D. M. F., and Crossthwaite, A. J. (2006) Higher-order organization and regulation of adenylyl cyclases, *Trends Pharmacol. Sci. 27*, 426−431.
54. McConnachie, G., Langeberg, L. K., and Scott, J. D. (2006) AKAP signaling complexes: getting to the heart of the matter, *Trends Mol. Med. 12*, 317−323.
55. Terrin, A., Di Benedetto, G., Pertegato, V., Cheung, Y.-F., Baillie, G., Lynch, M. J., Elvassore, N., Prinz, A., Herberg, F. W., Houslay, M. D., and Zaccolo, M. (2006) PGE_1 stimulation of HEK293 cells generates multiple contiguous domains with different [cAMP]: role of compartmentalized phosphodiesterases, *J. Cell. Biol. 175*, 441−451.
56. Zaccolo, M., and Pozzan, T. (2002) Discrete microdomains with high concentration of cAMP in stimulated rat neonatal cardiac myocytes, *Science 295*, 1711−1715.
57. Mongillo, M. (2004) Fluorescence resonance energy transfer-based analysis of cAMP dynamics in live neonatal rat cardiac myocytes reveals distinct functions of compartmentalized phosphodiesterases, *Circ. Res. 95*, 67−75.
58. Zmuda-Trzebiatowska, E., Oknianska, A., Manganiello, V., and Degerman, E. (2006) Role of PDE3B in insulin-induced glucose uptake, GLUT4 translocation and lipogenesis in primary rat adipocytes, *Cell. Signalling 18*, 382−390.
59. Bender, A. T., and Beavo, J. A. (2006) Cyclic nucleotide phosphodiesterases: Molecular regulation to clinical use, *Pharmacol. Rev. 58*, 488−520.
60. Omori, K., and Kotera, J. (2007) Overview of PDEs and their regulation, *Circ. Res. 100*, 309−327.
61. Liu. H., and Maurice, D. H. (1998) Expression of cyclic GMP-inhibited phosphodiesterases 3A and 3B (PDE3A and PDE3B) in rat tissues: differential subcellular localization and regulated expression by cyclic AMP, *Br. J. Pharmacol. 125*, 1501−1510.
62. Fujimoto, Y., Itabe, H., Kinoshita, T., Homma, K. J., Onoduka, J., and Mori, M. (2007) Involvement of ACSL in local synthesis of neutral lipids in cytoplasmic lipid droplets in human hepatocyte HuH7, *J. Lipid Res. 48*, 1280−1292.
63. Brasaemle, D. L., Dolios, G., Shapiro, L., and Wang, R. (2004) Proteomic analysis of proteins associated with lipid droplets of basal and lipolytically stimulated 3T3-L1 adipocytes, *J. Biol. Chem. 279*, 46835−46842.
64. Wang, H., Reaves, L. A., and Edens, N. K. (2006) Ginseng extract inhibits lipolysis in rat adipocytes in vitro by activating phosphodiesterase 4, *J. Nutr. 136*, 337−342.
65. Jepson, C. A., and Yeaman, S. J. (1992) Inhibition of hormone-sensitive lipase by intermediary lipid metabolites, *FEBS Lett. 310*, 197−200.
66. Hu, L., Deeney, J. T., Nolan, C. J., Peyot, M.-L., Ao, A., Richard, A. M., Luc, E., Faergeman, N. J., Knudsen, J., Guo, W., Sorhede-Winzell, M., Prentki, M., and Corkey, B. E. (2005) Regulation of lipolytic activity by long-chain acyl-coenyme A in islets and adipocytes, *Am. J. Physiol. Endocrinol. Metab. 289*, E1085−E1092.
67. Bader, S., Kortholt, A., and Van Haastert, P. J. M. (2007) Seven *Dictyostelium discoideum* phosphodiesterases degrade three pools of cAMP and cGMP, *Biochem. J. 402*, 153−161.
68. Zacher, L. A., and Carey, G. B. (1999) Cyclic AMP metabolism by swine adipocyte microsomal and plasma membranes, *Comp. Biochem. Physiol., Part B: Biochem. Mol. Biol. 124*, 61−71.
69. Nilsson, R., Ahmad, F., Swärd, K., Andersson, U., Weston, M., Manganiello, V., and Degerman, E. (2006) Plasma membrane cyclic nucleotide phosphodiesterase 3B (PDE3B) is associated with caveolae in primary adipocytes, *Cell. Signalling 18*, 1713−1721.

BI701413T